

A Magnetic Sensor for Hearing Aid Application

Crystal Carr, *Student Member, IEEE*

Department of Electrical and Computer Engineering, University of Maine

Abstract

This project consists of a integrated circuit that tests two amplifiers hooked up to an integrated telecoil, as well as several test amplifier circuits. The amplifiers are based on a single stage Cherry-Hooper configuration. The single stage Cherry Hooper design is simulated at a gain of 29 dB, THD of -50dB, and equivalent input noise of $2.01nV/\sqrt{(Hz)}$. The three stage Cherry Hooper design with filter is simulated at a gain of 84 dB, THD of -49dB, and equivalent input noise of $2.01nV/\sqrt{(Hz)}$. The three stage amplifier also has a bandwidth of 3kHz and a driving capacity of 30pF external load capacitance.

I. INTRODUCTION

A Magnetic sensor is desired that can detect changes in magnetic field. One application of this type of sensor is a telecoil in a hearing aid. A telecoil responds to magnetic field variations and not sound vibrations. This produces added clarity on telephones for hearing aid users as well as allowing them to enjoy the full effects of an opera or concert, assuming that the concert hall has an Inductive Loop (IL) system.

A telecoil consists of many loops of wire surrounding a permeable core. It relies on Faraday's Law of Induction¹ shown in Equation 1 to become a magnetic sensor. V is the voltage induced in the loop, \vec{E} is the electric field in the plane of the loop, dl is the small section of loop wire, and Ψ is the magnetic flux through the loop.

$$V = \oint \vec{E} \cdot dl = -\frac{\partial \Psi}{\partial t} \quad (1)$$

A telecoil or T-Coil generates an input signal for the hearing aid, similar to a microphone. Many types of hearing aids contain both microphones and telecoils to maximize convenience for hearing aid wearers. Instead of amplifying sound waves like the microphone, a telecoil amplifies the changes in magnetic field produced by a loop system or telephone speaker.

The changing magnetic field needed for hearing aid use is generated by a magnet in the speaker of a telephone or by an IL system. A changing voltage on a wire will create a changing magnetic flux inside the loop of wire. Therefore if the hearing aid user stands inside this loop, the telecoil in the hearing aid can pick up the changing magnetic flux generated by the IL system and translate it into an audio signal.

The voltage signal generated by the telecoil can be amplified and translated into an audio signal by placing the amplified voltage signal across the speaker in the hearing aid. By using a telecoil, ambient noise is minimized and the hearing aid user can hear telephone or concert more clearly.

The telecoil circuit is ideal for phone use, concert halls or anywhere a loudspeaker or public address (PA) system is used. In Europe (esp UK), concert halls have this type of system as a common service to their patrons. Concert halls in the US seem to rely on IR or FM communication systems which require bulky added equipment such as special microphones, speakers, and/or special headphones on each patron.

About 10% of the population would benefit from the use of hearing aides, and only 20% of those people who need them actually have hearing aides[1]. Two common obstacles to getting a hearing aid are cost and vanity. People often do not want to admit they want a hearing aid or they don't want other people to know that they need one.

Most hearing aides that contain telecoils are still made with hand wrapped wire telecoils. This feature increases the price and size of the hearing aide. Finding a way to implement a telecoil and low noise amplifier (LNA) amplifier in an integrated technology would allow lower cost and smaller size. Therefore the prices could decrease and the hearing aide itself could become more discrete, encouraging more of the population to get their needed hearing aides.

Figure 1 shows a common hearing aide configuration using a telecoil. An incoming signal causes sound and magnetic field in the telephone receiver. The telecoil receives the magnetic field vibrations. The signal from the telecoil is put through a LNA

¹The voltage induced in the wire of the telecoil is directly proportional to the rate of change of magnetic flux.

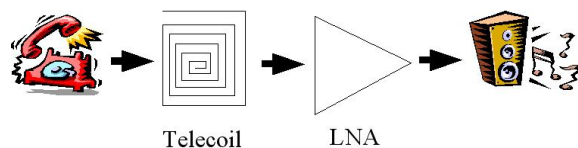


Fig. 1. Magnetic signal processing with telecoil circuit

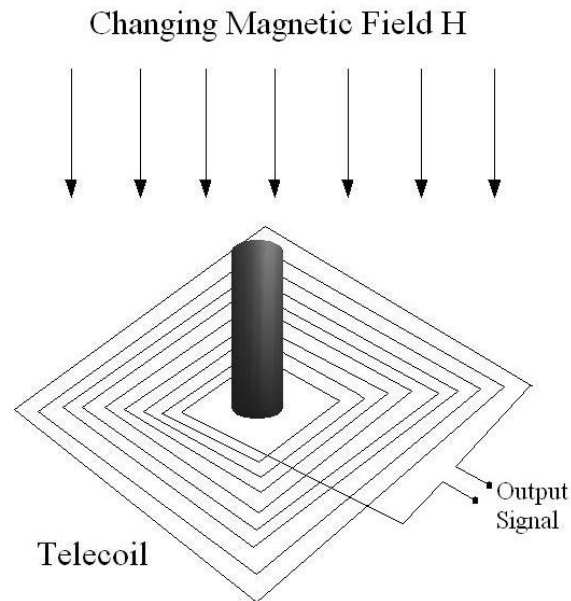


Fig. 2. Signal from changing magnetic flux

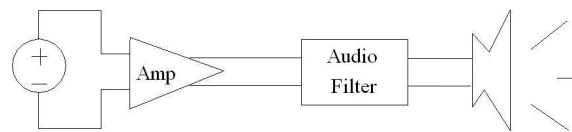


Fig. 3. Processing of telecoil output

and the result is sent through a speaker to a person's ear. This configuration reduces the noise incurred between source of sound and hearing aid user.

This project concentrates on the integration of a telecoil and LNA on a single integrated circuit. This combination is tailored to the audio range, fulfilling the need for the application of a hearing aid. A proper desired telecoil will maximize the inductance possible for the fabrication technology utilized as well as having a constant sheet resistance. The LNA should have constant amplification in the audio range and should have a low noise floor, on the order of -50dB.

II. CIRCUIT DESIGN

This project consists of a integrated circuit with two fully differentiable amplifiers hooked up to a telecoil, as well as several test amplifier circuits. The two amplifiers connected to the telecoil are static gain amplifiers. To offset this liability, they have different gain regions. Therefore, when testing, the range of gain actually needed in the device can be approximated. The test amplifiers are included to characterize the performance of the amplifier configuration as well as test structures for the main design in case unexpected behavior is observed.

A setup to test the chip is shown in Figure 2. A permeable core is placed in the center of the integrated telecoil. As the magnetic field changes, a voltage is induced across the coil. The magnitude of the induced voltage is dependent on several factors including material properties, geometry, frequency of vibration, and strength of magnetic field. To maximize the induced voltage this project uses a telecoil with as many turns as possible as well as a permeable material as a core to amplify the change in magnetic flux. Figure 3 shows that the induced voltage from the telecoil is then amplified, filtered, and placed across a speaker.

To obtain the best circuit design, iterative parametric simulations were used to obtain optimum configuration for gain performance while observing THD and noise analysis. The simple current mirror design was chosen for the current source because of its simplicity and stability in the audio spectrum. The Cherry Hooper amplifier Design [2] is a commonly used amplifier that seems to fit the project requirements. It consists of a two stage fully differential amplifier with passive feedback as shown in Figure 4. It is a transconductance to transimpedance amplifier that satisfies the project requirement to work with very small input signals. The resistances and transistors are matched which require special layout considerations. The multiple stage Cherry Hooper amplifiers in this design are decoupled with 5pF capacitors differentially.

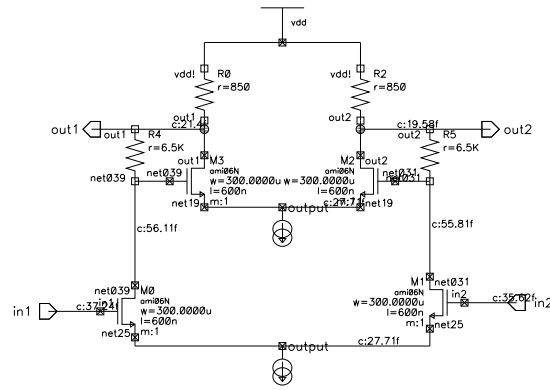


Fig. 4. Cherry Hooper Amplifier Schematic with Parasitics

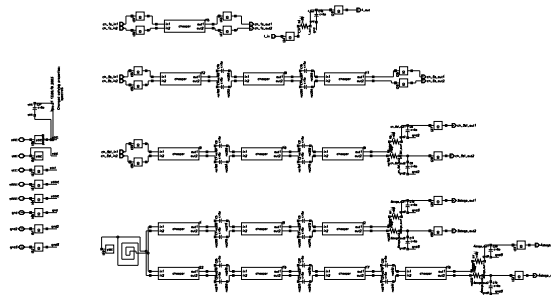


Fig. 5. Final Design Schematic

The output filter is a simple low-pass RC filter. It has an RC time constant of $0.25\mu s$ with a resistance of $5M\Omega$ and a capacitance of $5pF$.

Figure 5 shows the completed project schematic. The main project consists of a 3 stage and 4 stage amplifier connected to the telecoil and with filters. Several test circuits also exist including a stand-alone 3 stage amplifier with filter, a 3 stage amplifier without filter, a single stage amplifier, and a test filter. This will allow accurate debugging in the case of circuit failure. However, due to layout restrictions, complete simulations were only completed for the single stage test amplifier, and 3 stage test amplifier with filter.

III. CIRCUIT PERFORMANCE

All the simulations were performed at $37.78^\circ C$ because this is slightly greater than body temperature and is close to the operating temperature of a hearing aid. The input signal used has a frequency of 1kHz and a peak to peak amplitude of 1uV unless otherwise noted.

The current source was tested with a diode biased nmos transistor as a load. The current is measured at the output node with no additional load on the output. The current shown in Figure 6 results in an ideal current of approximately $795\mu A$ and with parasitics the current increases to $827\mu A$. Since gain performance is not critical to the design, a current source with this much parasitic dependence is acceptable for this project.

Figure 7 shows that the output has a bias voltage of 1.88V from the single stage amplifier. If this signal was attached to the next stage of a multiple stage amplifier, the outputs of the second stage would saturate. This bias is too high for the stages to be directly coupled. Therefore, decoupling capacitors of $5pF$ are added between stages to bring the common mode voltage back down to zero for the following input.

The 3 stage design was analyzed with worst case pins attached to the outputs. The model for the worst case pins was taken from the information provided by MOSIS. The three stage Cherry Hooper amplifier design uses 3 single stage blocks with

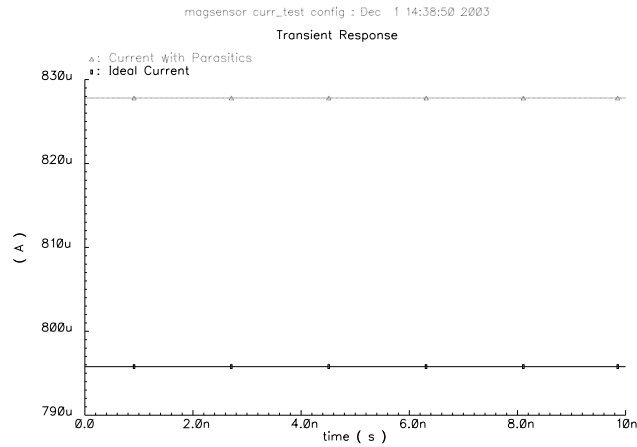


Fig. 6. Transient Performance

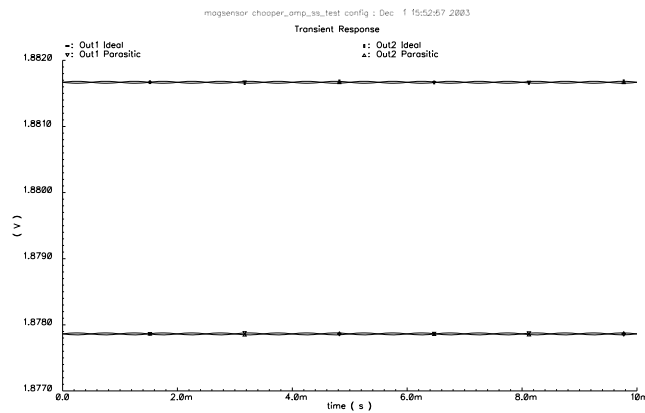


Fig. 7. Single Stage Cherry Hooper Biasing

decoupling capacitors between stages and a filter on the output. There are no decoupling capacitors on the output of the three stage amplifier, so therefore there is a final output bias of 1.88V shown in Figure 8.

Figure 9 shows the gain response of a single stage Cherry Hooper amplifier as a function of input signal peak to peak amplitude. The circuit will give 29 dB of gain up to a 10mV input signal before starting to saturate. The estimated input signal from the inductor is around $1\mu\text{V}$ and this circuit is linear for that region.

Figure 10 shows the three stage Cherry Hooper amplifier gain to be 84dB. This circuit is linear for input amplitudes up to $12\mu\text{V}$.

Figure 11 shows that the THD response of the single stage Cherry Hooper amplifier is at -50dB for inputs up to 1mV.

Figure 12 shows that the THD response of the three stage Cherry Hooper amplifier is approximately -50dB for inputs up to $10\mu\text{V}$.

Figure 13 shows the equivalent input noise of the single stage Cherry Hooper amplifier is $2.014nV/\sqrt{\text{Hz}}$. Over a frequency range of 10kHz, this would result in noise of about $0.2\mu\text{V}$.

Figure 14 shows the equivalent input noise of the three stage Cherry Hooper amplifier at $2.016nV/\sqrt{\text{Hz}}$, which is only slightly greater than the single stage noise.

The AC response of the three stage amplifier shown in Figure 15 shows that the 3dB point is at 3kHz, which will eliminate the high frequency noise on the output. This value is not the perfect choice for a hearing aid application which should not start attenuation until frequencies reach 5kHz or more. However, for this project it is sufficient and most of the testing will be done at 1kHz, which is not attenuated.

Figure 16 shows the gain of the three stage amplifier as a function of decoupling capacitance. The graph shows approximately

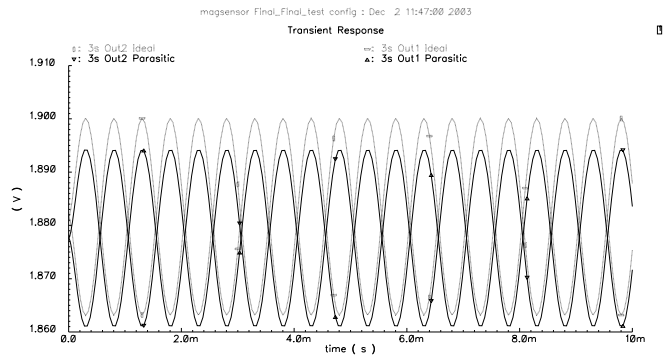


Fig. 8. Three Stage Cherry Hooper with Filter Biasing

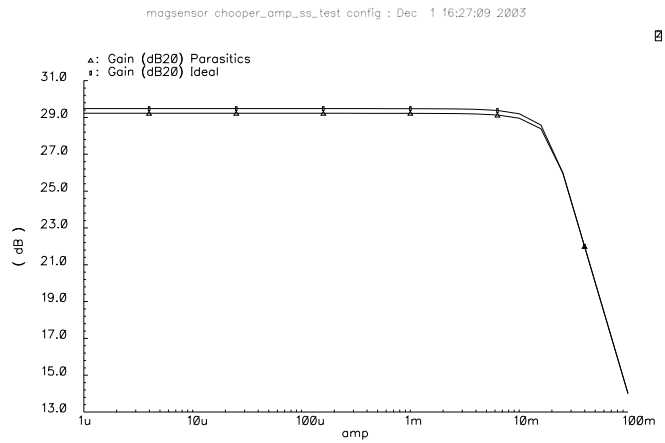


Fig. 9. Single Stage Cherry Hooper Gain Response

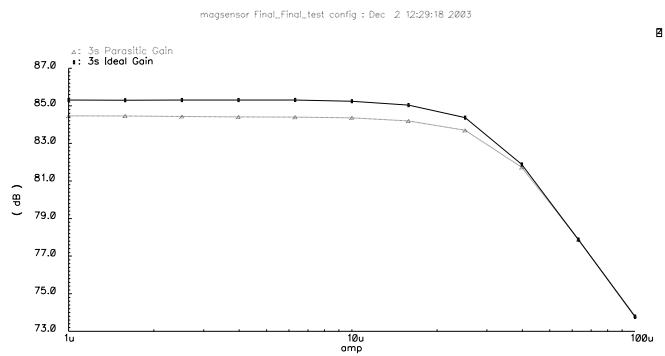


Fig. 10. Three Stage Cherry Hooper with Filter Gain Response

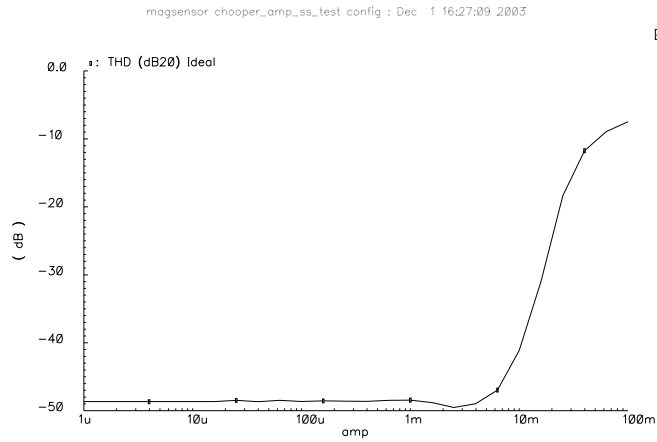


Fig. 11. Single Stage Cherry Hooper THD Response

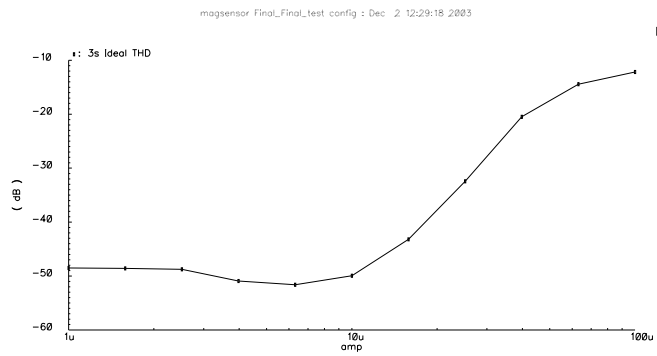


Fig. 12. Three Stage Cherry Hooper with Filter THD Response

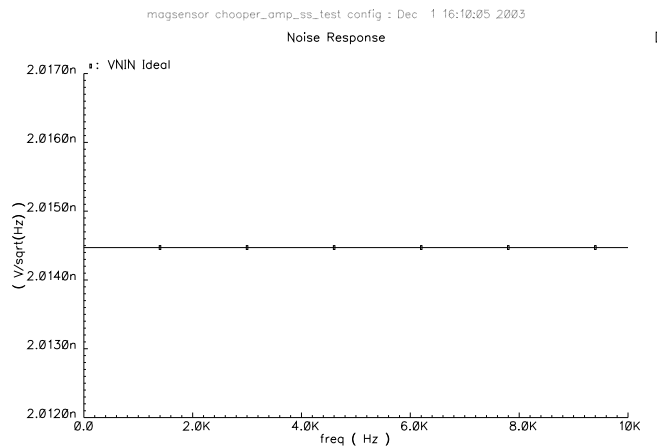


Fig. 13. Single Stage Cherry Hooper Noise Response

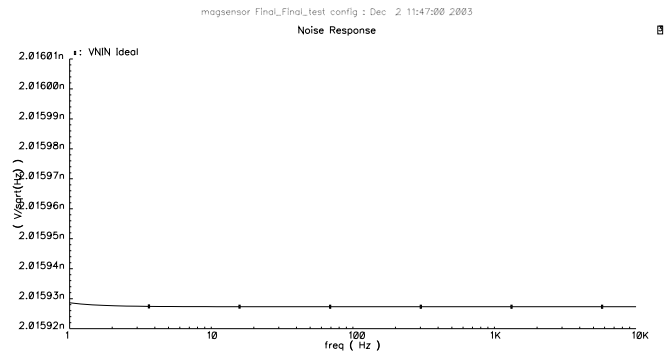


Fig. 14. 3Stage Cherry Hooper with Filter Noise Response

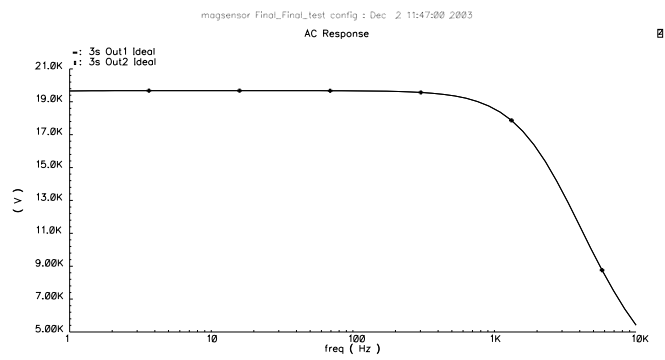


Fig. 15. 3Stage Cherry Hooper Amplifier with Filter AC Response

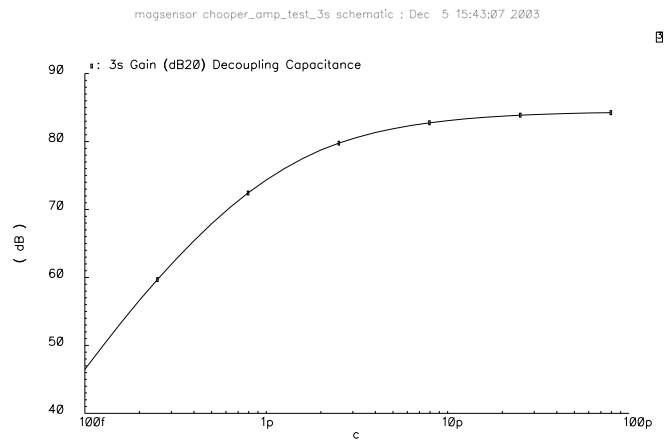


Fig. 16. Decoupling Capacitance between Stages

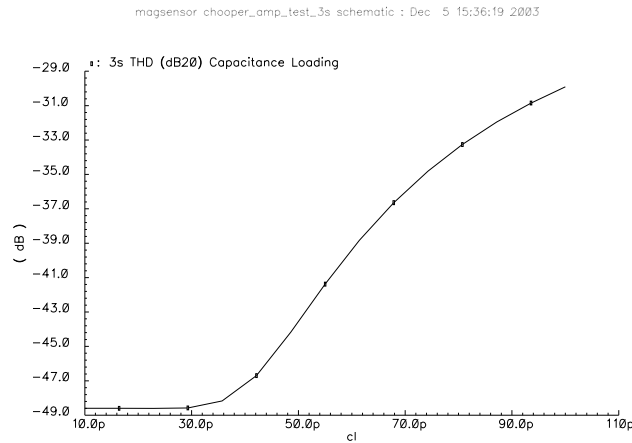


Fig. 17. Three Stage with Filter Drive Capability

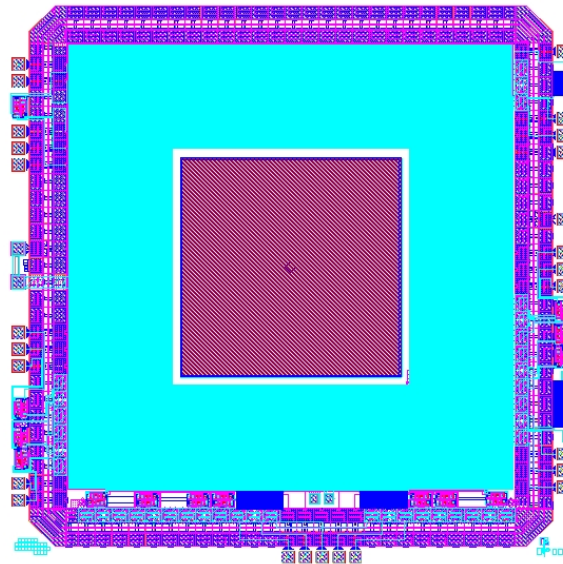


Fig. 18. Full Layout

maximum gain for decoupling capacitance of 10pF or greater. The tradeoff in this case is between layout size of the decoupling capacitors and overall gain performance of the amplifier. The value of 5pF was chosen to balance these two tradeoffs.

Figure 17 shows that no output buffer is needed on the circuit. The three stage amplifier with filter and worse case pins can drive an additional capacitance load of 30pF without sacrificing performance. The capacitance for the testing equipment for this project should be less than 30pF.

IV. PHYSICAL DESIGN

In a commercially available telecoil, the wire is wound around the permeable core, so that looking from the top, the wires are vertically stacked atop one another. In silicon design technology, there are a limited number of metal lines that can be stacked atop one another. In the AMI Semiconductor $0.5\mu m$ process, the maximum is three metal lines. In commercially available telecoils there are hundreds to thousands of metal loops around the core. The number of loops is directly proportional to magnetic response of the telecoil. Therefore, maximum possible number of turns is desired.

The integrated telecoil developed in this project uses all three possible metal layers. The bottom two metal layers are shorted together to create a sheet resistance equal to the top metal layer. The telecoil consists of many small loops that alternate between metal layers as the telecoil winds further out. This allows the loops to be stacked on one another as much as possible and allows the maximum amount of turns. The middle of the telecoil is left empty for a place to put the permeable core.

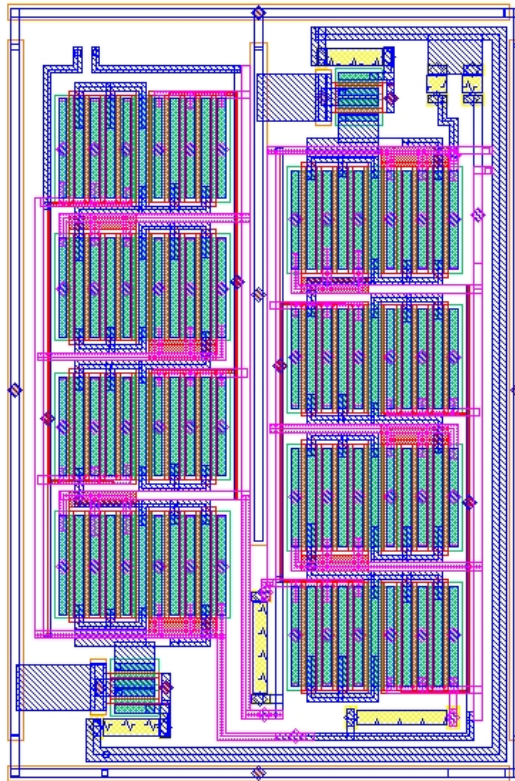


Fig. 19. Cherry Hooper Amplifier Layout

Device Type	Number
Nets	152
Terminals	26
Resistors	91
Capacitors	26
Pmos	26
Nmos	137
Inductor ²	1

TABLE I
DEVICE SUMMARY OF PROJECT

Figure 18 shows the full layout of the project including the telecoil. The total resistance of the telecoil is $34\text{k}\Omega$ and the capacitance is 238pF . Therefore the RC time constant of the telecoil is not something that is going to reduce the overall bandwidth of 3kHz .

The current source design takes up minimum space while ensuring ample contacts to substrate and power. There are two current sources in each Cherry Hooper single stage block. Figure 19 shows the layout of the single stage Cherry Hooper amplifier. This design uses the common centroid layout design to minimize variations in parasitics in matched transistors. All the other amplifier layouts as well as the project logo are located in Appendix I.

The telecoil is so large that it violates antenna rules. The top metal layer has an area of $1.11\text{e}6\mu\text{m}^2$. Therefore a fuse was created to tie the telecoil to ground during fabrication. Before testing begins the fuse line has to be hand scribed. Figure 20 shows the telecoil fuse layout.

Table IV shows a summary from Cadence of all the different types of devices in the project. Some of the numbers are misleading such as the number of resistors. When Cadence counted all the resistors, it counted each section of resistance. Some of the resistors in the project are one resistor made up of several small resistors (according to Cadence) in series. Also, the common centroid layout confused Cadence with the actual number of nmos transistors involved. Each transistor is broken up into four pieces with the common centroid layout and therefore Cadence sees four times more transistors than exist in the design. Also, the surge protection transistors in the guard ring count towards the total number of transistors displayed by Cadence.

Table IV shows a list of the major parasitics in the design. Most of the major parasitics are on pins of the device and

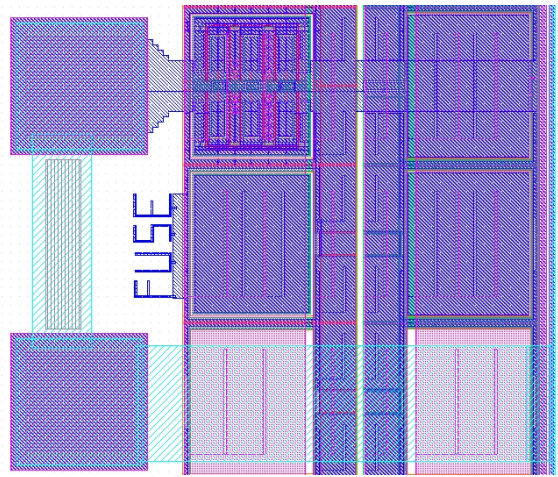


Fig. 20. Fuse Layout

Schematic Net	Capacitance Total
gnd3	5.442p
gnd2	3.074p
gnd	1.811p
4stage_out2	1.448p
3stage_out2	1.448p
3stage_out1	1.447p
4stage_out1	1.447p
ch_3sf_out2	1.378p
ch_3sf_out1	1.368p
f_out	1.348p
net274	1.196p
net248	1.19p
net250	1.189p
net240	1.188p
net246	1.186p
net270	1.18p
net276	1.176p
net244	1.17p
net242	1.169p
net272	1.162p
net195	1.158p
net194	1.155p
net198	1.155p
net199	1.154p
net187	1.147p
net207	1.146p
net206	1.142p
net186	1.14p

TABLE II
MAJOR PARASITICS IN FINAL LAYOUT

therefore can not be reduced by better design or layout techniques.

A copy of the pinout and bonding diagram can be found in Appendix II.

V. VERIFICATION

The final design passes DRC, LVS, electromigration rules, fill requirements and antenna rules (with the addition of the fuse).

The testing strategy has several steps. The first step will be to measure noise from the telecoil using the probe pads. Then the fuse will be cut allowing the telecoil to be able to respond to the magnetic signal. The inductance of the telecoil can at this point be measured. The permeable core needs to be placed exactly in the center of the chip. The test magnetic field will be generated and power provided allowing the outputs of the amplifiers to be observed.

If the output is too noisy, the magnetic field strength can be increased to determine a signal above the noise. Different cores should be tested to find the one with the best performance.

If the output is saturated, the field strength can be lowered to get an acceptable wave pattern. If the amplifiers are not responding, the test structures can be powered up to debug the circuits.

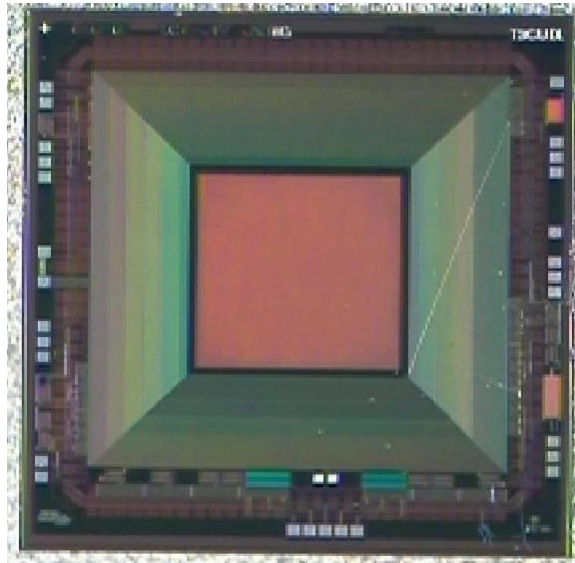


Fig. 21. Picture of Fabricated Design

VI. EXPERIMENTAL RESULTS

Figure 21 shows a picture of the fabricated design. There are a few shallow surface scratches and an inclusion that seems to be below the surface. The inclusion could be causing a short or open, or it could be harmless.

The resistance of the telecoil has been confirmed at $34k\Omega$. However, the resistance is too high for the Precision LCR meter to measure the inductance.

Characterization of the test amplifiers is currently in progress. When the test amplifiers are completely analyzed, the telecoil will be tested to see if it works.

VII. SUMMARY AND CONCLUSIONS

The current source provides 0.8mA. Therefore the estimated power consumption with all the external powers attached will be 112 mW. With only just the circuits attached to the telecoil powered, the estimated power consumption decreases by half to 56mW.

The single stage Cherry Hooper design has a simulated gain of 29 dB, THD of -50dB, and equivalent input noise of $2.01nV/\sqrt{(Hz)}$. The three stage Cherry Hooper design with filter has a simulated gain of 84 dB, THD of -49dB, and equivalent input noise of $2.01nV/\sqrt{(Hz)}$. The three stage amplifier also has a bandwidth of 3kHz and a driving capacity of 30pF external load capacitance.

Possible improvements for the future include extending the inductor into a process with 6 metal layers. This will greatly increase the inductance of the telecoil and increase the voltage signal from the telecoil.

One possible limitation of the Cherry Hooper amplifier is that there is no common mode feedback in the design. If this was part of the design, the decoupling capacitors would not be needed and the amplifier would increase in stability. Another limitation of the Cherry Hooper amplifier is that it does not perform well with a low source voltage[3] and therefore to make this design marketable a new low noise amplifier would have to be designed. It would also be beneficial for the amplifier to be variable gain[4] to allow consumer adjustment of volume.

Eventually it would be ideal to deposit the permeable core directly onto the silicon substrate. Magnetic materials have previously been deposited for use as printing heads[5] and therefore it could possibly be extending to non-magnetic permeable materials as well.

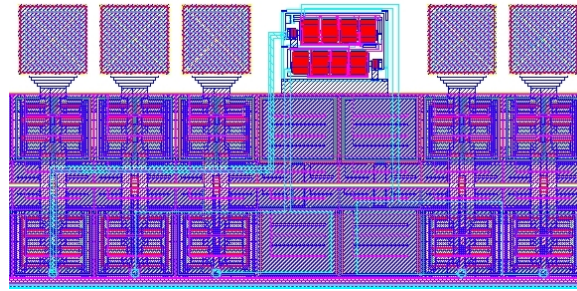


Fig. 22. Test Single Stage Layout

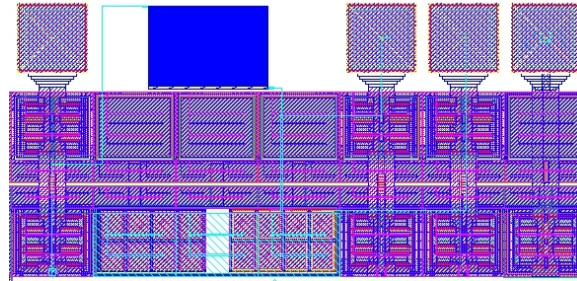


Fig. 23. Test Filter Layout



Crystal Carr Crystal Carr is currently a first year Master's candidate for Electrical Engineering at the University of Maine. Her undergraduate degrees include a B.S. in Engineering Physics and a B.S. in Computer Engineering, both from the University of Maine. At the conclusion of her Master's degree, she plans on pursuing a Doctorate in Electrical Engineering.

REFERENCES

- [1] Hear-It AISBL. Hear-it. Internet: <http://www.hear-it.org>, September 2003.
- [2] Mattias Dahlstrom Yun Wei Navin Parthasarathy Zachary Griffith, Krishnan Sundararajan and Mark J. W. Rodwell. 80 gb/sec tdm based fiber ics designs using ucsb's inp dhbt technology. Project report for micro project 00-083, Department of Electrical and Computer Engineering, University of California, University of California, Santa Barbara, California, 93106, 2001.
- [3] Behzad Razavi. Prospects of cmos technology for high-speed optical communication circuits. *IEEE Journal of Solid-State Circuits*, 37(9):1135–1145, September 2002.
- [4] Reinhard Steiner Christian C. Enz Jörg Hauptmann, Franz Dielacher and Fancois Krummenacher. A low-noise amplifier with automatic gain control and anticlipping control in cmos technology. *IEEE Journal of Solid-State Circuits*, 27(7):974–981, July 1992.
- [5] M. Bogdanski F. Cardot, J. Gobet and F. Rudolf. Fabrication of a magnetic transducer compsed of a high-density array of microelectromagnets with on-chip electronics. *Sensors and Actuators A*, 43:11–16, 1994.

APPENDIX I PHYSICAL LAYOUT

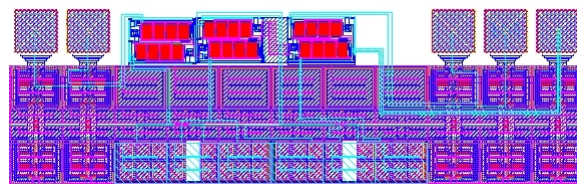


Fig. 24. Test Three Stage Layout

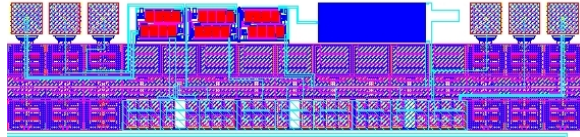


Fig. 25. Test Three Stage with Filter Layout

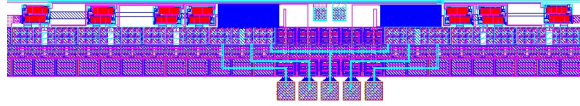


Fig. 26. Telecoil Three Stage and Four Stage Layout

APPENDIX II PINOUT & BONDING DIAGRAM

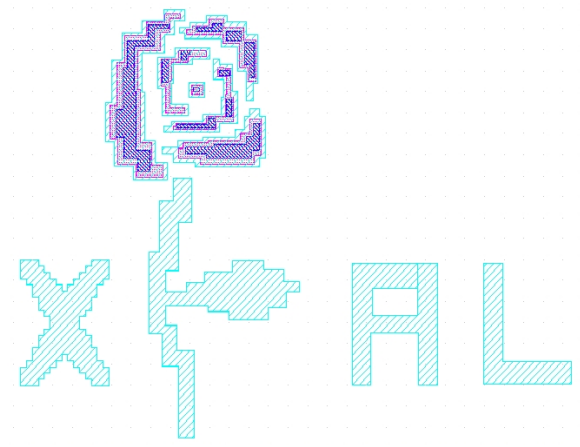


Fig. 27. Logo

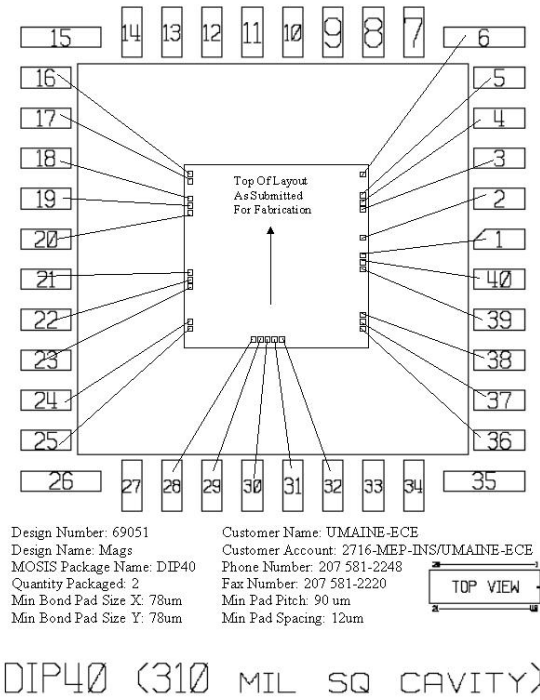


Fig. 28. Bonding Diagram

Name of Pin	I/O	Pin Number
4stage_out1	Output	28
4stage_out2	Output	29
3stage_out1	Output	32
3stage_out2	Output	31
ch_1s_out1	Output	17
ch_1s_out2	Output	16
ch_3s_out1	Output	25
ch_3s_out2	Output	24
ch_3sf_out1	Output	37
ch_3sf_out2	Output	38
ch_1s_in1	Input	18
ch_1s_in2	Input	19
ch_3s_in1	Input	22
ch_3s_in2	Input	23
ch_3sf_in1	Input	40
ch_3sf_in2	Input	39
f_out	Output	5
f_in	Input	6
gnd	I/O	4
gnd2	I/O	36
gnd3	I/O	30
vcc	I/O	20
vdd	I/O	3
vdda	I/O	21
vddd	I/O	1
vss	I/O	2

TABLE III
 PINOUT TABLE